Available online at www.sciencedirect.com
ScienceDirect
Computers & Fluids 35 (2006) 1217–1227
computers & fluids
www.elsevier.com/locate/compfluid

Examination of characteristics method with cubic interpolation for advection–diffusion equation

Tung-Lin Tsai [a,*], Shih-Wei Chiang [b], Jinn-Chuang Yang [b]

[a] *Natural Hazard Mitigation Research Center, National Chiao Tung University, 1001 Ta Hsueh Road, Hsinchu 30010, Taiwan, ROC*
[b] *Department of Civil Engineering, National Chiao Tung University, 1001 Ta Hsueh Road, Hsinchu 30010, Taiwan, ROC*

Received 6 August 2004; received in revised form 11 May 2005; accepted 26 August 2005
Available online 24 October 2005

Abstract

In this study, the use of the characteristics method integrated with the Hermite cubic interpolation or the cubic-spline interpolation on the space line or the time line, i.e., the HCSL scheme, the CSSL scheme, the HCTL scheme, and the CSTL scheme, respectively, for solving the advection–diffusion equation is examined. The advection and diffusion of a Gaussian concentration distribution in a uniform flow with constant diffusion coefficient is used to conduct this investigation. The effects of parameters, such as Peclet number, Courant number, and the reachback number, on these four schemes used herein for solving the advection–diffusion equation are investigated. The simulated results show that the CSSL scheme is comparable to the HCSL scheme, and the two schemes seem insensitive to Courant number as compared with the HCTL scheme and the CSTL scheme. With large Peclet number, for small Courant number the HCTL scheme is more accurate than the HCSL scheme and the CSSL scheme. However, for large Courant number the HCTL scheme has worse computed results in comparison with the HCSL scheme and the CSSL scheme. With small Peclet number, the HCTL scheme, the HCSL scheme, and the CSSL scheme have close simulated results. Despite Peclet number, for small Courant number the CSTL scheme is comparable to the HCTL scheme, but for large Courant number the former scheme provides unacceptable simulated results in which very large numerical diffusion is induced due to the effect of the natural endpoint constraint. For large Peclet number the HCSL scheme and the CSSL scheme integrated with the reachback technique can improve simulated results, but for small Peclet number the HCSL scheme and the CSSL scheme seem not to be influenced by increasing the reachback number.
© 2005 Elsevier Ltd. All rights reserved.

1. Introduction

Modeling the advection and diffusion of contaminants in natural water bodies, such as rivers, lakes, oceans, and groundwater, has become very important in recent years due to the increasing awareness of the effects of pollutants on human health and aquatic life. Among various numerical schemes used for solving the advection–diffusion equation, the split-operator approach in which the advection and diffusion processes are separately computed using different numerical schemes has been pursued by many numerical modelers. In the split-operator approach, the diffusion process can be accurately computed by several numerical schemes, such as the Crank–Nicholson central difference scheme, the Crank–Nicholson Galerkin finite element scheme, and some others. Hence, the accuracy of solving the advection–diffusion equation will mainly be related to the simulated results of the advection process.

It is well known that the method of characteristics has many advantages for the theoretical and physical interpretation of the advection process. The method of characteristics can be classified into two categories. One is the characteristics-grid scheme, and the other is the fixed-grid scheme. The former has the potential to give accurate solution, but its grid system is awkward

* Corresponding author. Tel.: +886 3 5131468; fax: +886 3 5734116.
E-mail address: tltsai@mail.nctu.edu.tw (T.-L. Tsai).

0045-7930/$ - see front matter © 2005 Elsevier Ltd. All rights reserved.
doi:10.1016/j.compfluid.2005.08.002

Notation

The following symbols are used in this paper:

A, B, C, D, E, F, G, H, a_1–a_4 and b_1–b_4	coefficients for interpolation
C_r	Courant number
m	reachback number
P_e	Peclet number
R	second derivative with respect to time
S	second derivative with respect to space
U	flow velocity component
ε	diffusion coefficient
Φ	concentration
Φ_x	first derivative of Φ with respect to space
Φ_t	first derivative of Φ with respect to time
σ	standard deviation
Δx	computational grid interval
Δt	time increment

Subscript

i	x-directional computational point index

Superscript

n	time step index

for practical applications. The latter then has been a popular scheme due to the convenience of numerical simulation. With the fixed-grid scheme, the characteristic trajectory usually does not pass through the grid points. An interpolation technique can be applied to obtain corresponding values at the foot of the trajectory in terms of the neighboring grid points. Thus, the form of interpolation technique will largely affect the accuracy of the fixed-grid scheme.

The characteristics method integrated with the Hermite cubic interpolation, which is called HC method in this study, was first proposed to solve the advection equation by Holly and Preissmann [1]. The HC method is based on the construction of cubic interpolating polynomials in terms of the dependent variable and its first derivative for two adjacent points on the spatial axis. In order to increase the availability of the HC method, some extensions of the HC method have been presented [2–4]. The technique of the characteristic trajectory outward [2] or backward [3] on the spatial axis was applied to the original HC method. The former relaxes the constraint of Courant number less than unity in the original HC method. The Courant number can be expressed as $C_r = U\Delta t/\Delta x$ in which U is flow velocity. Δx and Δt are the grid size and the time step, respectively. In addition, the latter allows the characteristic trajectory to project back beyond the present time level to increase the computational accuracy. Furthermore, a concept of extending the characteristic trajectory backward on the temporal axis has also been employed to the HC method by Yang and Hsu [4], in which the space-line interpolation used in the original HC method is replaced by the time-line interpolation. In this paper, applying the HC method to the space line and the time line are respectively termed the 'HCSL scheme' and the 'HCTL scheme'. Yang and Hsu [4] showed that the HCTL scheme is more accurate than the HCSL scheme when Courant number is less than unity. However, for Courant number larger than unity the HCSL scheme has better simulated results as compared with the HCTL scheme.

As mentioned above, the first derivatives of the dependent variable with respect to space or time are needed for the application of the HC method. Thus, in order to obviate the need to solve the spatial or temporal derivatives of the auxiliary equation, an alternative cubic-spline interpolation function was employed to solve the advection–diffusion equation by Schohl and Holly [5], Karpik and Crokett [6], and Stefanovic and Stefan [7]. The application of the cubic-spline interpolation, originally developed on the space line, was extended to the time line by Ahmad and Kothyari [8]. In this study, the characteristics method integrated with cubic-spline interpolation on the space line and the time line are denoted as the 'CSSL scheme' and the 'CSTL scheme', respectively.

The HCSL scheme, the HCTL scheme, the CSSL scheme, and the CSTL scheme had been presented for many years, but had never been compared in details. The goal of this study is to examine the use of these four schemes for solving the advection–diffusion equation. In the following sections, the numerical frameworks of these four schemes investigated herein are first briefly reviewed. Modeling the advection and diffusion of a Gaussian concentration distribution is then used to investigate the computational performances of the HCSL scheme, the HCTL scheme, the CSSL scheme, and the CSTL scheme. It must be noticed that since the characteristics method integrated with cubic interpolation on both space and time lines may not be applicable to the problems with high gradient, especially the problems with infinite slope such as a step function [7,11], a Gaussian concentration distribution with considerable width is used for the examination.

2. Numerical framework of characteristics method with cubic interpolation for advection–diffusion equation

The one-dimensional advection–diffusion equation for a conservative material can be expressed as

$$\frac{\partial \Phi}{\partial t} + U\frac{\partial \Phi}{\partial x} = \varepsilon\frac{\partial^2 \Phi}{\partial x^2} \tag{1}$$

where the scalar function $\Phi(x,t)$ represents concentration at position x and time t with uniform flow velocity U and constant diffusion coefficient ε.

Eq. (1) can be rewritten in terms of total derivative, i.e., $\mathrm{d}/\mathrm{d}t$, as

$$\frac{\mathrm{d}\Phi}{\mathrm{d}t} = \varepsilon\frac{\partial^2 \Phi}{\partial x^2} \tag{2}$$

along the characteristic curve

$$\frac{\mathrm{d}x}{\mathrm{d}t} = U \tag{3}$$

Integrating (2) and (3) along the characteristic curve from l to p shown in Figs. 1 and 2 yields

$$\Phi_i^{n+1} = \Phi_l + \varepsilon\int_{t_l}^{t_p}\frac{\partial^2 \Phi}{\partial x^2}\,\mathrm{d}t \tag{4}$$

and

$$x_p - x_l = U(t_p - t_l) \tag{5}$$

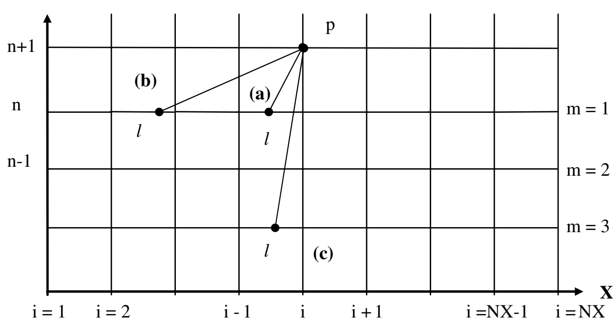

Fig. 1. The schematic diagram of space-line interpolation: (a) classical case, (b) reachout case, and (c) reachback case.

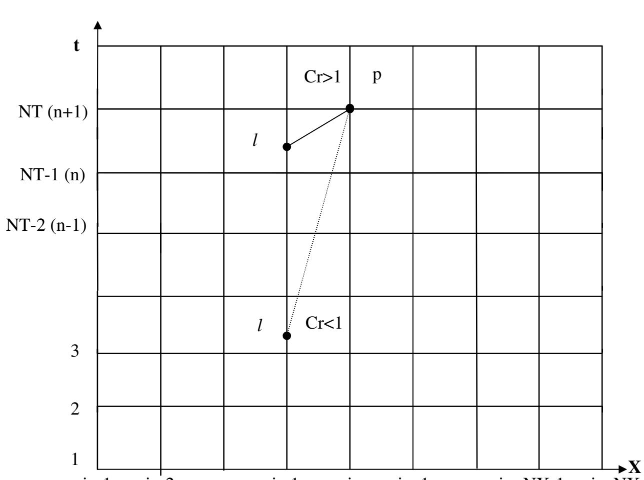

Fig. 2. The schematic diagram of time-line interpolation (solid line: $C_r > 1$, dash line: $C_r < 1$).

By applying the characteristics method, the advection–diffusion equation shown in (1) is replaced by (4) and (5). The foot of the characteristic trajectory, i.e., x_l, falls on the space line shown in Fig. 1. Since x_l usually does not coincide with the grid points, the interpolation technique should be used to approximate Φ_l. Depending on the foot of the characteristic trajectory, three cases can occur in the space-line interpolation, i.e., the classical case, the reachout case, and the reachback case. The classical case shown in Fig. 1(a), originally proposed by Holly and Preissmann [1], appears when Courant number is less than unity and the characteristic curve intersects on the space line within a grid size at the current time level. If Courant number is larger than unity, the characteristic trajectory can fall on the spatial axis outside of a grid size at the present time level as shown in Fig. 1(b). This is the so-called reachout case [2]. The reachback case, shown in Fig. 1(c), occurs when the characteristic curve projects on the space line beyond the present time level. In addition, the characteristic trajectory can also be allowed to intersect on the time line instead of the space line [4,8] shown in Fig. 2 to approximate Φ_l.

In the following, the uses of the characteristics method with the Hermite cubic interpolation or the cubic-spline interpolation on the space line or the time line, i.e., the HCSL scheme, the HCTL scheme, the CSSL scheme, and the CSTL scheme, for solving the advection–diffusion equation shown in (4) and (5) are briefly reviewed.

2.1. The HCSL scheme

The major idea of the Hermite cubic interpolation is to construct a cubic polynomial function between two grid points with the dependent variable and its first derivative. When the characteristic trajectory intersects on the space line shown in Fig. 1, Φ_l can be approximated by using the Hermite cubic interpolation as follows:

$$\Phi_l = a_1\Phi_{i-\hat{n}-1}^{n+1-m} + a_2\Phi_{i-\hat{n}}^{n+1-m} + a_3\Phi_{xi-\hat{n}-1}^{n+1-m} + a_4\Phi_{xi-\hat{n}}^{n+1-m} \tag{6}$$

with

$$\hat{n} = \mathrm{INT}\frac{mU\Delta t}{\Delta x} \tag{7}$$

where m is reachback number shown in Fig. 1. INT denotes the integral portion of $mU\Delta t/\Delta x$. The superscript and subscript of Φ represent the time level and the grid node, respectively. Φ_x is the first derivative of Φ with respect to space. The coefficients a_1–a_4 in (6) are displayed in Appendix I. Eq. (6) can represent the original, reachout, and reachback cases. With $m = 1$, $\hat{n} = 0$ and $\hat{n} \geqslant 1$ are respectively the original case and the reachout case. $m > 1$ represents the reachback case.

Applying the trapezoidal-rule approximation for calculation of integration and the second-order central difference scheme for discretization of the diffusion process, the time integration term shown on the right-hand side of (4) becomes

$$\int_{t_l}^{t_p} \frac{\partial^2 \Phi}{\partial x^2}\,\mathrm{d}t = \frac{m\Delta t}{2}\left(\frac{\Phi_{i-1}^{n+1} - 2\Phi_i^{n+1} + \Phi_{i+1}^{n+1}}{\Delta x^2} + \frac{\Phi_{i-\hat{n}-1}^{n+1-m} - 2\Phi_{i-\hat{n}}^{n+1-m} + \Phi_{i-\hat{n}+1}^{n+1-m}}{\Delta x^2}\right) \tag{8}$$

An additional equation for solving Φ_x appearing in (6) can be obtained by taking the spatial derivative of (1) as follows:

$$\frac{\partial \Phi_x}{\partial t} + U\frac{\partial \Phi_x}{\partial x} = \varepsilon \frac{\partial^2 \Phi_x}{\partial x^2} \tag{9}$$

One can clearly see from (1) and (9) that Φ_x and Φ have the same form of governing equation, i.e., the advection–diffusion equation. Thus, Φ_x can be solved by following the concept similar to that used for solving Φ as shown in (4) and (5). Using the Hermite cubic interpolation, the first derivative of Φ with respect to space at the foot of characteristic trajectory, i.e., Φ_{xl}, can be represented as

$$\Phi_{xl} = b_1\Phi_{i-\hat{n}-1}^{n+1-m} + b_2\Phi_{i-\hat{n}}^{n+1-m} + b_3\Phi_{x_i-\hat{n}-1}^{n+1-m} + b_4\Phi_{x_i-\hat{n}}^{n+1-m} \tag{10}$$

where the coefficients b_1–b_4 are shown in Appendix I. In addition, the diffusion portion of Φ_x, similar to Φ, can be computed by use of (8) with replacing Φ by Φ_x.

2.2. The HCTL scheme

Like the HCSL scheme as mentioned above, applying the Hermite cubic interpolation to the time line for solving the advection–diffusion equation requires an auxiliary equation of Φ_t that can be obtained by taking the temporal derivative of (1) as follows:

$$\frac{\partial \Phi_t}{\partial t} + U\frac{\partial \Phi_t}{\partial x} = \varepsilon \frac{\partial^2 \Phi_t}{\partial x^2} \tag{11}$$

Φ_l and Φ_{tl}, i.e., Φ and Φ_t at foot of characteristic trajectory on the time line, shown in Fig. 2 can be approximated by use of the Hermite cubic interpolation as follows:

$$\Phi_l = a_1\Phi_{i-1}^{n-\hat{m}} + a_2\Phi_{i-1}^{n+1-\hat{m}} + a_3\Phi_{ti-1}^{n-\hat{m}} + a_4\Phi_{ti-1}^{n+1-\hat{m}} \tag{12}$$

and

$$\Phi_{tl} = b_1\Phi_{i-1}^{n-\hat{m}} + b_2\Phi_{i-1}^{n+1-\hat{m}} + b_3\Phi_{ti-1}^{n-\hat{m}} + b_4\Phi_{ti-1}^{n+1-\hat{m}} \tag{13}$$

with

$$\hat{m} = \mathrm{INT}\frac{\Delta x}{U\Delta t} \tag{14}$$

where the forms of the coefficients a_1–a_4 and b_1–b_4 shown in (12) and (13) are exactly the same as those shown in (6) and (10). The details of the minor differences are given in Appendix I.

In the HCTL scheme, the time integration term of the diffusion process shown on the right-hand side of (4), similar to the concept used for the HCSL scheme, can be evaluated as

$$\int_{t_l}^{t_p} \frac{\partial^2 \Phi}{\partial x^2}\,\mathrm{d}t = \frac{\hat{m}\Delta t}{2}\left(\frac{\Phi_{i-1}^{n+1} - 2\Phi_i^{n+1} + \Phi_{i+1}^{n+1}}{\Delta x^2} + \frac{\Phi_{i-2}^{n+1-\hat{m}} - 2\Phi_{i-1}^{n+1-\hat{m}} + \Phi_i^{n+1-\hat{m}}}{\Delta x^2}\right) \tag{15}$$

In addition, the diffusion process of Φ_t can also be solved by use of (15) with Φ_t instead of Φ.

2.3. The CSSL scheme

The cubic-spline interpolation is to construct a piecewise cubic polynomial function of dependent variable between two nodes (grid points) with the satisfaction of the fact that the interpolating function must pass through each node and be continuous in its first and second derivatives at interior nodes. In the cubic-spline interpolation, the nodal slopes can be computed by the condition that a piecewise cubic interpolation should be twice continuously differentiable so that the interpolation function has a continuous curvature. Therefore, the major difference between the cubic-spline interpolation and the Hermite cubic interpolation is that the former need not deal with additional equations for spatial or temporal derivatives, whereas the latter need do that.

One can employ the characteristics method integrated with the cubic-spline interpolation for solving the advection–diffusion equation shown in (4) and (5). When the characteristic trajectory falls on the space line shown in Fig. 1, the diffusion process, like the HCSL scheme, can be computed by the use of (8). In addition, Φ_l can be approximated by the cubic-spline interpolation as follows:

$$\Phi_l = A_{i-\hat{n}-1}^{n+1-m}[(1-\omega)\Delta x]^3 + B_{i-\hat{n}-1}^{n+1-m}[(1-\omega)\Delta x]^2 + C_{i-\hat{n}-1}^{n+1-m}[(1-\omega)\Delta x] + D_{i-\hat{n}-1}^{n+1-m} \tag{16}$$

with

$$\omega = \frac{mU\Delta t}{\Delta x} - \hat{n} \tag{17}$$

where $\hat{n}$ is given by (7). The coefficients shown in (16), i.e., $A_{i-\hat{n}-1}^{n+1-m}$, $B_{i-\hat{n}-1}^{n+1-m}$, $C_{i-\hat{n}-1}^{n+1-m}$, and $D_{i-\hat{n}-1}^{n+1-m}$, can be written as

$$A_{i-\hat{n}-1}^{n+1-m} = \frac{S_{i-\hat{n}}^{n+1-m} - S_{i-\hat{n}-1}^{n+1-m}}{6\Delta x} \tag{18}$$

$$B_{i-\hat{n}-1}^{n+1-m} = \frac{S_{i-\hat{n}-1}^{n+1-m}}{2} \tag{19}$$

$$C_{i-\hat{n}-1}^{n+1-m} = \frac{\Phi_{i-\hat{n}}^{n+1-m} - \Phi_{i-\hat{n}-1}^{n+1-m}}{\Delta x} - \frac{2\Delta x S_{i-\hat{n}-1}^{n+1-m} + \Delta x S_{i-\hat{n}}^{n+1-m}}{6} \tag{20}$$

$$D_{i-\hat{n}-1}^{n+1-m} = \Phi_{i-\hat{n}-1}^{n+1-m} \tag{21}$$

where S_j^{n+1-m} denotes the second derivative with respect to space at grid point j and time level $n+1-m$, and it can be obtained by applying the continuity of the first derivative with respect to space [9,10] as follows:

$$S_{j-1}^{n+1-m} + 2S_j^{n+1-m} + S_{j+1}^{n+1-m} = \frac{6}{\Delta x^2}\left(\Phi_{j+1}^{n+1-m} - 2\Phi_j^{n+1-m} + \Phi_{j-1}^{n+1-m}\right), \quad j = 2,\ldots,NX-1 \tag{22}$$

where 1 and NX respectively represent the two endpoints, i.e., the left and right boundaries, shown in Fig. 1. The system of (22) is underdetermined due to only $NX-2$ equations for finding NX unknowns. Two additional endpoint constraints for S_1^{n+1-m} and S_{NX}^{n+1-m} are required to close this system. The natural constraint is frequently used with neglect of the second derivatives at endpoints, i.e., $S_1^{n+1-m} = S_{NX}^{n+1-m} = 0$ [5–7].

2.4. The CSTL scheme

If the characteristic trajectory intersects on the time line shown in Fig. 2, Φ_l, similar to the CSSL scheme, could be also evaluated by use of the cubic-spline interpolation on the time line as follows:

$$\Phi_l = E_{i-1}^{n-\hat{m}}[(1-\zeta)\Delta t]^3 + F_{i-1}^{n-\hat{m}}[(1-\zeta)\Delta t]^2 + G_{i-1}^{n-\hat{m}}[(1-\zeta)\Delta t] + H_{i-1}^{n-\hat{m}} \tag{23}$$

with

$$\zeta = \frac{\Delta x}{U\Delta t} - \hat{m} \tag{24}$$

where $\hat{m}$ is shown in (14). The coefficients $E_{i-1}^{n-\hat{m}}$, $F_{i-1}^{n-\hat{m}}$, $G_{i-1}^{n-\hat{m}}$, and $H_{i-1}^{n-\hat{m}}$ in (23), similar to those from the CSSL scheme, are displayed in Appendix II. Like the CSSL scheme, the natural endpoint constraint, shown in (40) and (41) appearing in Appendix II, is also applied to the use of the cubic-spline interpolation on the time line [8]. In addition (15) used for the HCTL scheme, can also be applied to calculate the diffusion process for the CSTL scheme.

3. Demonstration and evaluation

Modeling the advection and diffusion of a Gaussian concentration distribution in a uniform flow with constant diffusion coefficient is used herein to investigate the computational performances of the HCSL scheme, the HCTL scheme, the CSSL scheme, and the CSTL scheme. With the initial condition as follows:

$$\Phi(x) = \exp\left[\frac{-(x-x_0)^2}{2\sigma^2}\right] \tag{25}$$

the well-known exact solution of (1) is

$$\Phi(x,t) = \frac{\sigma}{\sqrt{\sigma^2+2\varepsilon t}}\exp\left[\frac{-(x-x_0-Ut)^2}{2(\sigma^2+2\varepsilon t)}\right] \tag{26}$$

where σ is the standard deviation of Gaussian distribution. x_0 is the peak position of Gaussian distribution in the initial time.

A grid size of 100 m and a time step of 100 s are used to conduct this simulation. The peak position of Gaussian distribution is at $x_0 = 1400$ m. In this simulation, the domain is long enough so that the boundary effect can be ignored, i.e., neglect of Φ, Φ_x, and Φ_t at the boundaries. The effects of parameters, such as Courant number (C_r), the reachback number (m), and Peclet number ($P_e = U\Delta x/\varepsilon$), on these four schemes used herein for solving the advection–diffusion equation are examined. For a reachback number larger than unity, the HCSL scheme and the CSSL scheme need to set up the additional initial conditions. For example, with the reachback number of 3, the two additional initial conditions at first and second time steps, except the initial condition at the beginning time shown in (25), are required to conduct the simulation. In this study, the exact solution shown in (26) is applied to obtain the additional initial conditions. In addition, for the HCTL scheme and the CSTL scheme with Courant number less than unity the exact solution is also used to obtain the additional initial conditions. In the following, the pure advection of a Gaussian distribution concentration is first used to examine the computational performances of the HCSL scheme, the CSSL scheme, the HCTL scheme, and the CSTL scheme. The comparisons of simulated results by the advection and diffusion of a Gaussian distribution concentration from these four schemes are then conducted.

3.1. Calculation of pure advection

3.1.1. Effect of Courant number

The computed results in terms of the maximum and minimum values as well as the rms (root mean square) errors from the HCSL scheme, the CSSL scheme, the HCTL scheme, and the CSTL scheme with different flow velocities of 0.3 m/s, 0.7 m/s, and 1.4 m/s, and different standard deviations of 100 m, 150 m, and 250 m for 100 time steps calculation are shown in Table 1. Fig. 3 shows the exact solution and the simulated results from various numerical schemes with standard deviation of 150 m and different flow velocities. In this case, Peclet number is infinite due to only consideration of advection process without the diffusion process. Three different Courant numbers of 0.3, 0.7, and 1.4 which are respectively less than, close to, and larger than unity are used in this simulation. It can be observed from Table 1 that these four schemes have better simulated results with

Table 1
Computational performances of various schemes in pure advection test

Schemes			Concentrations		
			Max.	Min.	rms error
$\sigma = 100$ m	$C_r = 0.3$	HCSL	0.7920	−0.0323	0.0194
		CSSL	0.7592	−0.0682	0.0238
		HCTL	0.9983	0	0.0001
		CSTL	0.9971	0	0.0001
	$C_r = 0.7$	HCSL	0.7921	−0.0322	0.0192
		CSSL	0.7593	−0.0683	0.0237
		HCTL	0.9236	−0.0048	0.0067
		CSTL	0.8931	−0.1878	0.0334
	$C_r = 1.4$	HCSL	0.7832	−0.0312	0.0202
		CSSL	0.7395	−0.0548	0.0253
		HCTL	0.6109	−0.0468	0.0376
		CSTL	0.2410	−0.0148	0.0835
$\sigma = 150$ m	$C_r = 0.3$	HCSL	0.9193	−0.0083	0.0087
		CSSL	0.9066	−0.0183	0.0106
		HCTL	0.9996	0	0.0001
		CSTL	0.9997	0	0.0001
	$C_r = 0.7$	HCSL	0.9194	−0.0084	0.0086
		CSSL	0.9065	−0.0183	0.0107
		HCTL	0.9789	−0.0002	0.0021
		CSTL	1.0258	−0.0891	0.0208
	$C_r = 1.4$	HCSL	0.9139	−0.0089	0.0092
		CSSL	0.8923	−0.0102	0.0120
		HCTL	0.7865	−0.0337	0.0244
		CSTL	0.3505	−0.0152	0.0772
$\sigma = 250$ m	$C_r = 0.3$	HCSL	0.9847	0	0.0020
		CSSL	0.9845	0	0.0020
		HCTL	1.0000	0	0.0001
		CSTL	1.0000	0	0.0001
	$C_r = 0.7$	HCSL	0.9846	0	0.0020
		CSSL	0.9845	0	0.0021
		HCTL	0.9968	0	0.0004
		CSTL	1.0485	−0.0033	0.0094
	$C_r = 1.4$	HCSL	0.9832	0	0.0021
		CSSL	0.9804	0	0.0025
		HCTL	0.9382	0	0.0084
		CSTL	0.5328	0	0.0703

large standard deviation of Gaussian distribution. In addition, for different standard deviations, the same conclusions from the simulated results of these four schemes seem to be reached.

From Fig. 3 and Table 1, the HCSL scheme and the CSSL scheme have comparable simulated results in which some degree of numerical diffusion and oscillation occurs. For small Courant number the computed results from the HCTL scheme are very close to the exact solution. Thus, the HCTL scheme is more accurate than the HCSL scheme and the CSSL scheme. However, when Courant number is large the HCTL scheme gives large numerical diffusion and oscillation than the HCSL scheme and the CSSL scheme. In addition, with small Courant number, the simulated results from the CSTL scheme are close to those from the HCTL scheme. However, for large Courant number the CSTL scheme has unacceptable simulated results in which very large numerical diffusion is induced. As mentioned above, it can be concluded that the HCSL scheme and the CSSL scheme seem insensitive to Courant number as compared with the HCTL scheme and the CSTL scheme. In other words, the computed results from the HCTL scheme and the CSTL scheme are strongly related to Courant number, especially the latter.

With small Courant number, the HCTL scheme and the CSTL scheme are better than the HCSL scheme and

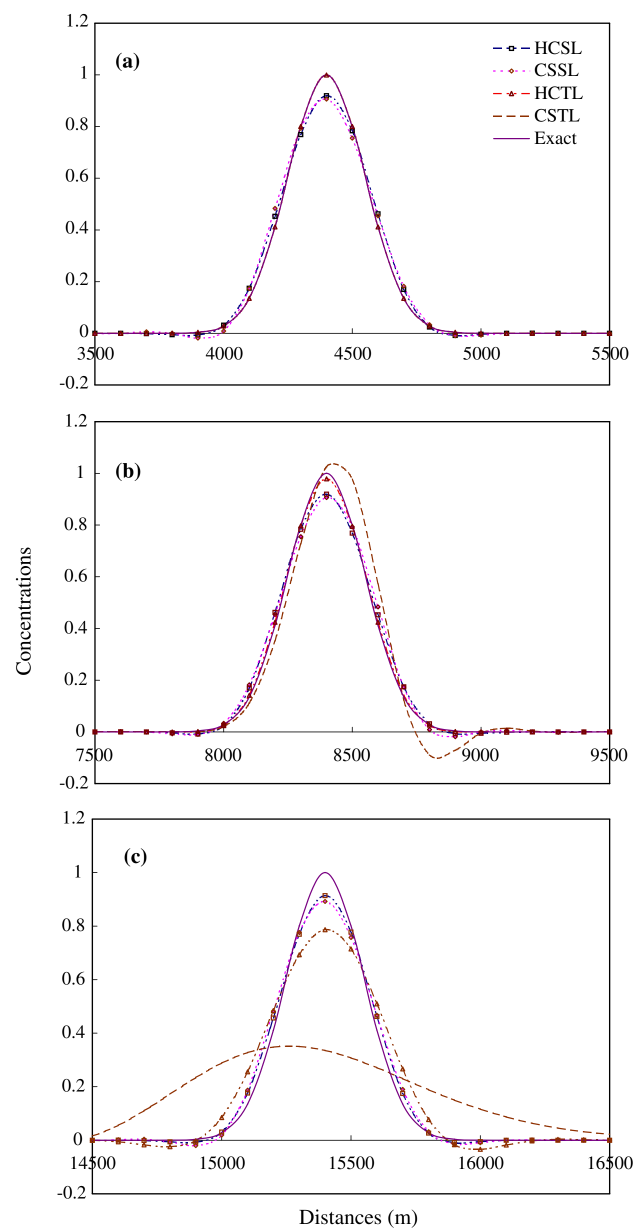

Fig. 3. The simulated results of pure advection test for different schemes with $\sigma = 150$ m. (a) $C_r = 0.3$; (b) $C_r = 0.7$; (c) $C_r = 1.4$.

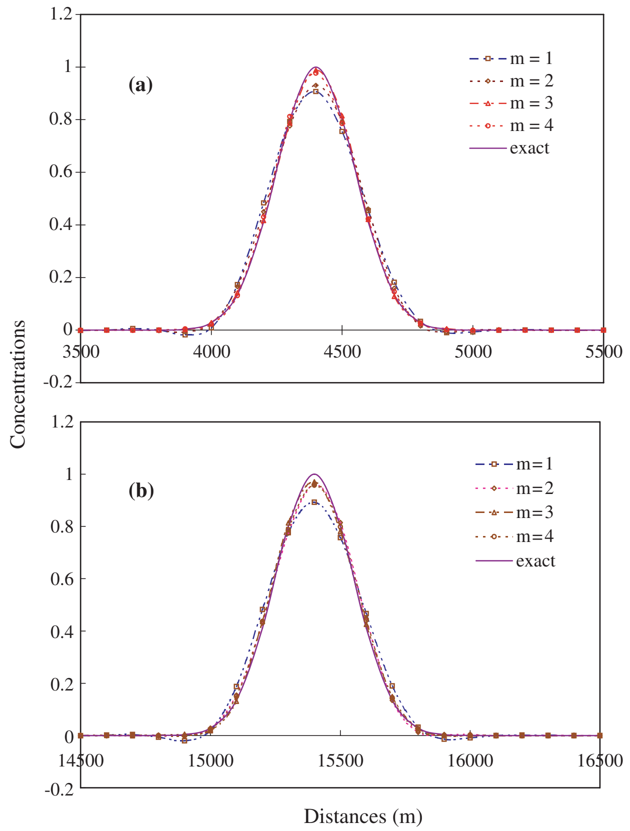

Fig. 4. The simulated results of pure advection test by the CSSL scheme with $\sigma = 150$ m and different reachback numbers. (a) $C_r = 0.3$; (b) $C_r = 1.4$.

the CSSL scheme. However, it must be noticed that the characteristic trajectory of the HCTL scheme and the CSTL scheme will project back far away from the current time level to intercept the time line while Courant number is too small, for example Courant number less than 0.1. This may be inconvenient to the additional initial condition preparation and program coding. Thus, for too small Courant number, it seems suitable to apply the HCSL scheme and the CSSL scheme rather than the HCTL scheme and the CSTL scheme.

3.1.2. Note on endpoint constraint effect

As shown in Table 1 and Fig. 3, with large Courant number, the CSTL scheme provides unconvincing simulated results that have very large numerical diffusion in comparison with the other three schemes. This may be due to the use of natural endpoint constraint for the cubic-spline interpolation on the time line. The natural cubic-spline interpolation neglects the second derivative at endpoint shown in (40) and (41), which makes the end cubics approach linearity at their extremities. With small Courant number, the foot of characteristic trajectory will be far from the endpoints, i.e., grid points at time level $n + 1$, shown in Fig. 2, so that the effect of endpoint constraint could be ignored. However, when Courant number is large the natural endpoint constraint will significantly influence the computed results due to the foot of characteristic trajectory close to the endpoints. It must be noticed that Tsai et al. [10] examined the effect of natural endpoint constraint on the cubic-spline interpolation applied to the space line. They pointed out that in spite of little numerical diffusion convincing simulated results are obtained. Thus, one may conclude that for the cubic-spline interpolation, the effect of natural endpoint constraint on the time line is more significant than that on the space line.

3.1.3. Effect of reachback number

The simulated results from the HCSL scheme and the CSSL scheme with standard deviation of 150 m, different flow velocities of 0.3 m/s and 1.4 m/s, and different reachback numbers are shown in Figs. 4, 5 and Tables 2, 3, respectively. One can find from Figs. 4, 5 and Tables 2, 3 that the HCSL scheme and the CSSL scheme are comparable, and their simulated results are improved with the reachback technique. The best computed results are obtained when the reachback number is 3. With the reachback number larger than 3, the accuracy of the simulated results seems not to be increased. One must notice that the characteristics method with the reachback technique can indeed improve the

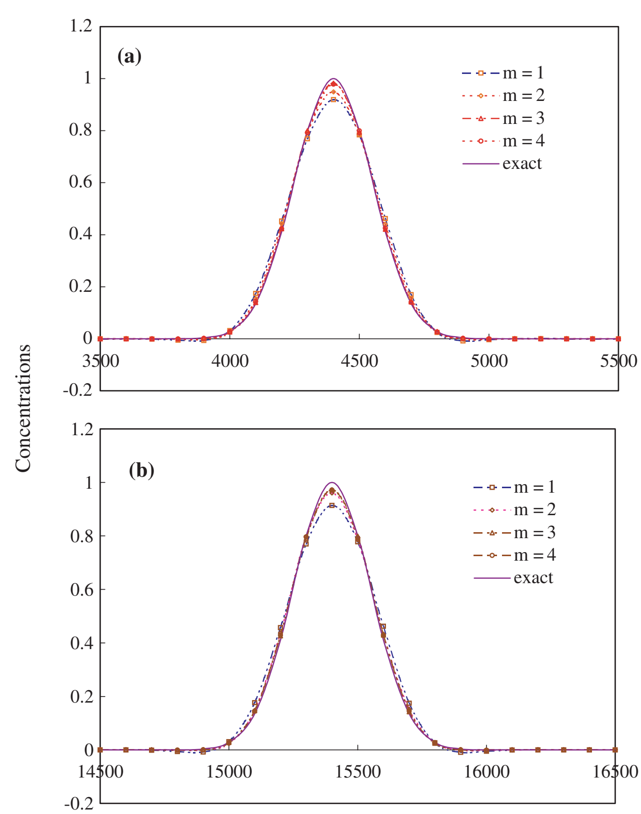

Fig. 5. The simulated results of pure advection test by the HCSL scheme with $\sigma = 150$ m and different reachback numbers. (a) $C_r = 0.3$; (b) $C_r = 1.4$.

Table 2
Simulated results of pure advection test by the CSSL scheme with $\sigma = 150$ m and different reachback numbers

Schemes		Concentrations		
		Max.	Min.	rms error
$C_r = 0.3$	$m = 1$	0.9193	−0.0083	0.0221
	$m = 2$	0.9492	−0.0025	0.0135
	$m = 3$	0.9825	−0.0003	0.0045
	$m = 4$	0.9785	−0.0005	0.0056
$C_r = 1.4$	$m = 1$	0.9139	−0.0089	0.0235
	$m = 2$	0.9603	−0.0016	0.0105
	$m = 3$	0.9724	−0.0084	0.0072
	$m = 4$	0.9717	−0.0073	0.0073

Table 3
Simulated results of pure advection test by the HCSL scheme with $\sigma = 150$ m and different reachback numbers

Schemes		Concentrations		
		Max.	Min.	rms error
$C_r = 0.3$	$m = 1$	0.9066	−0.0183	0.0270
	$m = 2$	0.9380	−0.0076	0.0191
	$m = 3$	0.9882	−0.0001	0.0049
	$m = 4$	0.9870	−0.0002	0.0051
$C_r = 1.4$	$m = 1$	0.8923	−0.0202	0.0305
	$m = 2$	0.9590	−0.0014	0.0126
	$m = 3$	0.9708	−0.0008	0.0090
	$m = 4$	0.9680	−0.0013	0.0103

accuracy of the simulated results, but it may be not easy to set up the additional initial conditions and to decide the best reachback number, especially for the simulation of complicated flow patterns, such as in open channel flow computation [11].

3.2. Calculation of advection and diffusion

3.2.1. Effects of Courant and Peclet numbers

The advection and diffusion of a Gaussian concentration distribution is further used to examine the computational performances of the HCSL scheme, the CSSL scheme, the HCTL scheme, and the CSTL scheme. Like the calculation of pure advection, three representative Courant numbers of 0.3, 0.7, and 1.3 are used in this simulation. In order to examine the influence of different Peclet numbers, each flow velocity is used with different diffusion coefficients of 0.5 m^2/s and 10 m^2/s. Thus, for the case of Courant number of 1.3, the two different Peclet numbers are 260 and 13. Peclet numbers are 140 and 7 or 60 and 3 when Courant numbers are 0.7 and 0.3, respectively. Three different standard deviations of 100 m, 150 m, and 250 m are employed to examine the effects of different gradient concentrations on various schemes. The computed results in terms of the maximum and minimum values as well as the rms errors from these four schemes for 100 time steps calculation are shown in Tables 4 and 5. Fig. 6 shows the exact solution and the computed results using various numerical schemes with standard deviation of 150 m and different flow velocities, and two different diffusion coefficients.

It can be found from Fig. 6 and Tables 4, 5 that the HCSL scheme and the CSSL scheme have comparable computed results. With small diffusion coefficient, i.e., large Peclet number, the HCTL scheme and the CSTL scheme are better than the HCSL scheme and the CSSL scheme while Courant number is small. However, for large Courant number the simulated results from the

Table 4
Simulated results of various schemes in advection and diffusion test with $\varepsilon = 0.5$ m^2/s

Schemes			Concentrations		
			Max.	Min.	rms error
$\sigma = 100$ m	$C_r = 0.3$	HCSL	0.6440	−0.0093	0.0071
$C_{\max} = 0.7071$	$P_e = 60$	CSSL	0.6397	−0.0115	0.0074
		HCTL	0.7312	0	0.0023
		CSTL	0.7310	0	0.0023
	$C_r = 0.7$	HCSL	0.6637	−0.1155	0.0067
	$P_e = 140$	CSSL	0.6385	−0.0250	0.0097
		HCTL	0.7092	0	0.0026
		CSTL	0.7413	−0.0741	0.0150
	$C_r = 1.3$	HCSL	0.6227	−0.0111	0.0091
	$P_e = 260$	CSSL	0.6397	−0.0115	0.0073
		HCTL	0.5904	−0.0184	0.0128
		CSTL	0.2850	−0.0225	0.0698
$\sigma = 150$ m	$C_r = 0.3$	HCSL	0.7955	−0.0022	0.0046
$C_{\max} = 0.8320$	$P_e = 60$	CSSL	0.7962	−0.0034	0.0041
		HCTL	0.8419	0	0.0012
		CSTL	0.8421	0	0.0011
	$C_r = 0.7$	HCSL	0.8111	−0.0067	0.0048
	$P_e = 140$	CSSL	0.7973	−0.0032	0.0061
		HCTL	0.8334	0	0.0017
		CSTL	0.8877	−0.0327	0.0126
	$C_r = 1.3$	HCSL	0.7775	−0.0031	0.0065
	$P_e = 260$	CSSL	0.7962	−0.0034	0.0042
		HCTL	0.7550	−0.0123	0.0093
		CSTL	0.4095	−0.0181	0.0559
$\sigma = 250$ m	$C_r = 0.3$	HCSL	0.9175	0	0.0017
$C_{\max} = 0.9285$	$P_e = 60$	CSSL	0.9203	0	0.0012
		HCTL	0.9306	0	0.0003
		CSTL	0.9308	0	0.0004
	$C_r = 0.7$	HCSL	0.9259	0	0.0022
	$P_e = 140$	CSSL	0.9217	0	0.0021
		HCTL	0.9289	0	0.0007
		CSTL	0.9738	−0.0006	0.0077
	$C_r = 1.4$	HCSL	0.9080	0	0.0029
	$P_e = 260$	CSSL	0.9202	0	0.0011
		HCTL	0.9036	−0.0015	0.0037
		CSTL	0.6029	−0.0027	0.0508

Note: $C_{\max}$ represents the maximum value of concentration obtained from exact solution.

Table 5
Simulated results of various schemes in advection and diffusion test with $\varepsilon = 10\ m^2/s$

Schemes			Concentrations		
			Max.	Min.	rms error
$\sigma = 100$ m	$C_r = 0.3$	HCSL	0.2188	0	0.0009
$C_{max} = 0.2182$	$P_e = 3$	CSSL	0.2191	0	0.0010
		HCTL	0.2196	0	0.0004
		CSTL	0.2196	0	0.0004
	$C_r = 0.7$	HCSL	0.2193	0	0.0023
	$P_e = 7$	CSSL	0.2189	0	0.0022
		HCTL	0.2197	0	0.0010
		CSTL	0.2240	0	0.0011
	$C_r = 1.3$	HCSL	0.2180	0	0.0010
	$P_e = 13$	CSSL	0.2191	0	0.0009
		HCTL	0.2206	0	0.0031
		CSTL	0.1812	0	0.0080
$\sigma = 150$ m	$C_r = 0.3$	HCSL	0.3188	0	0.0013
$C_{max} = 0.3180$	$P_e = 3$	CSSL	0.3191	0	0.0013
		HCTL	0.3198	0	0.0005
		CSTL	0.3199	0	0.0005
	$C_r = 0.7$	HCSL	0.3193	0	0.0031
	$P_e = 7$	CSSL	0.3188	0	0.0030
		HCTL	0.3198	0	0.0013
		CSTL	0.3259	0	0.0016
	$C_r = 1.3$	HCSL	0.3177	0	0.0013
	$P_e = 13$	CSSL	0.3191	0	0.0013
		HCTL	0.3210	0	0.0043
		CSTL	0.2664	0	0.0112
$\sigma = 250$ m	$C_r = 0.3$	HCSL	0.4888	0	0.0016
$C_{max} = 0.4879$	$P_e = 3$	CSSL	0.4893	0	0.0016
		HCTL	0.4900	0	0.0007
		CSTL	0.4900	0	0.0006
	$C_r = 0.7$	HCSL	0.4900	0	0.0038
	$P_e = 7$	CSSL	0.4893	0	0.0038
		HCTL	0.4901	0	0.0016
		CSTL	0.4979	0	0.0021
	$C_r = 1.3$	HCSL	0.4875	0	0.0016
	$P_e = 13$	CSSL	0.4894	0	0.0016
		HCTL	0.4906	0	0.0053
		CSTL	0.4185	0	0.0154

Note: C_{max} represents the maximum value of concentration obtained from exact solution.

HCTL scheme and the CSTL scheme are worse than those of the HCSL scheme and the CSSL scheme, especially the CSTL scheme inducing very large numerical diffusion. The conclusions of various schemes for solving the advection–diffusion equation with small diffusion coefficient, as mentioned above, seem similar to those from the calculation of pure advection equation.

In contrast, with large diffusion coefficient, i.e., small Peclet number, no matter what the Courant number is, the HCSL scheme, the CSSL scheme, and the HCTL

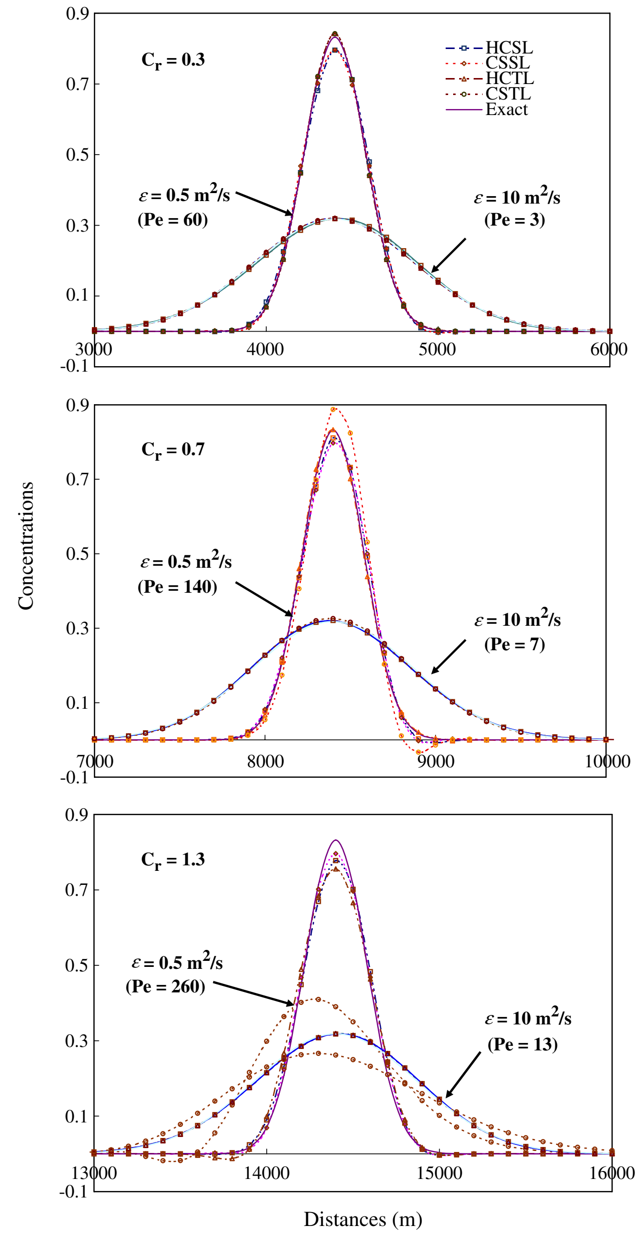

Fig. 6. The simulated results of advection and diffusion test for different schemes with $\sigma = 150$ m.

scheme have close computed results that approach the exact solution. The outcome mentioned above can also be applied to the CSTL scheme with small Courant number. However, when Courant number is large the CSTL scheme provides poor computed results in which very large numerical diffusion is induced. One can again see that the CSTL scheme is significantly sensitive to Courant number due to the natural endpoint constraint.

The simulated results from the HCSL scheme and the CSSL scheme with standard deviation of 150 m, flow velocity of 1.3 m/s, two different diffusion coefficients of 0.5 m^2/s and 10 m^2/s, and different reachback numbers for 100 time steps calculation are shown in Fig. 7.

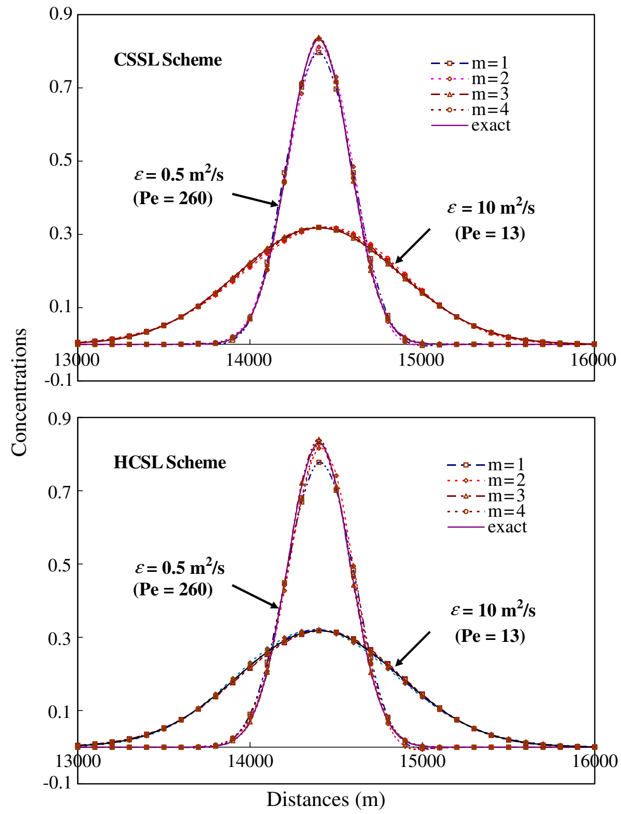

Fig. 7. The simulated results of advection and diffusion test with $C_r = 1.3$, $\sigma = 150$ m, and different reachback numbers.

From Fig. 7, one can see that with the reachback technique the accuracy of the HCSL scheme and the CSSL scheme increases when Peclet number is large. However, for small Peclet number the HCSL scheme and the CSSL scheme integrated with the reachback technique seems not to improve the simulated results.

4. Conclusions

The advection and diffusion of a Gaussian concentration distribution in a uniform flow with constant diffusion coefficient is used to investigate the computational performances of the HCSL scheme, the CSSL scheme, the HCTL scheme, and the CSTL scheme. From the simulated results of these four schemes examined herein, one may conclude the following:

1. The CSSL scheme is comparable to the HCSL scheme, and both provide convincing computed results in spite of some degree of numerical diffusion and oscillation.
2. The HCSL scheme and the CSSL scheme seem insensitive to Courant number, but the HCTL scheme and the CSTL scheme strongly depend on Courant number, especially the latter.
3. With large Peclet number, for small Courant number the HCTL scheme has better computed results than the HCSL scheme and the CSSL scheme. However, for large Courant number the simulated results from the HCTL scheme are worse than those of the HCSL scheme and the CSSL scheme. With small Peclet number these three schemes produce close simulated results regardless of Courant number.
4. For small Courant number, the CSTL scheme is comparable to the HCTL scheme, but for large Courant number the CSTL scheme provides poor simulated results suffering from very large numerical diffusion, as compared with the HCTL scheme. This may be because that the natural endpoint constraint is used for the cubic-spline interpolation on the time line.
5. Since they obviate the need to deal with the additional equations for spatial or temporal derivatives, the CSSL scheme and the CSTL scheme are easier to implement and more efficient than the HCSL scheme and the HCTL scheme.
6. For large Peclet number, the simulated results from the HCSL scheme and the CSSL scheme are improved with the reachback technique. However, for small Peclet number the HCSL scheme and the CSSL scheme are not sensitive to the reachback number.

Appendix I. Coefficients of the Hermite cubic interpolation

$$a_1 = \theta^2(3 - 2\theta) \tag{27}$$

$$a_2 = 1 - a_1 \tag{28}$$

$$a_3 = \theta^2(1 - \theta)\Delta x \tag{29}$$

$$a_4 = -\theta(1 - \theta)^2\Delta x \tag{30}$$

$$b_1 = 6\theta(\theta - 1)/\Delta x \tag{31}$$

$$b_2 = -b_1 \tag{32}$$

$$b_3 = \theta(3\theta - 2) \tag{33}$$

$$b_4 = (\theta - 1)(3\theta - 1) \tag{34}$$

In the space-line interpolation, θ equals $(mU\Delta t/\Delta x) - \hat{n}$, and $\hat{n}$ is shown in (7). In the time-line interpolation, θ is $(\Delta x/U\Delta t) - \hat{m}$ in which $\hat{m}$ is given by (14), and Δx shown in (29)–(31) needs to be replaced by Δt.

Appendix II. Coefficients of the cubic-spline interpolation on the time line

$$E_{i-1}^{n-\hat{m}} = \frac{R_{i-1}^{n+1-\hat{m}} - R_{i-1}^{n-\hat{m}}}{6\Delta t} \tag{35}$$

$$F_{i-1}^{n-\hat{m}} = \frac{R_{i-1}^{n-\hat{m}}}{2} \tag{36}$$

$$G_{i-1}^{n-\hat{m}} = \frac{\Phi_{i-1}^{n+1-\hat{m}} - \Phi_{i-1}^{n-\hat{m}}}{\Delta t} - \frac{2\Delta t R_{i-1}^{n-\hat{m}} + \Delta t R_{i-1}^{n+1-\hat{m}}}{6} \tag{37}$$

$$H_{i-1}^{n-\hat{m}} = \Phi_{i-1}^{n-\hat{m}} \tag{38}$$

where $R_{i-1}^{n-\hat{m}}$, second derivative for Φ with respect to time at grid point $i-1$ and time level $n-\hat{m}$, could be expressed as following relation

$$R_{i-1}^{k-1} + 2R_{i-1}^{k} + R_{i-1}^{k+1} = \frac{6}{\Delta t^2}\left(\Phi_{i-1}^{k-1} - 2\Phi_{i-1}^{k} + \Phi_{i-1}^{k+1}\right),$$
$$k = 2, 3, \ldots, n \tag{39}$$

According to the natural cubic-spline interpolation, two additional constraints for second derivative with respect to time at initial time level and time level $n+1$, i.e., R_{i-1}^{1} and R_{i-1}^{n+1}, could be represented as

$$R_{i-1}^{1} = 0 \tag{40}$$

and

$$R_{i-1}^{n+1} = 0 \tag{41}$$

References

[1] Holly Jr FM, Preissmann A. Accurate calculation of transport in two dimensions. J Hydr Div 1977;103:1259–77.
[2] Yang JC, Wang JY. Numerical solution of dispersion in one dimension. J Chin Inst Eng 1988;11:379–83.
[3] Yang JC, Hsu EL. On the use of the reach-back characteristics method for calculation of dispersion. Int J Numer Methods Fluids 1991;12:225–35.
[4] Yang JC, Hsu EL. Time-line interpolation for solution of the dispersion equation. J Hydraul Res 1990;28:503–20.
[5] Schohl GA, Holly Jr FM. Cubic-spline interpolation in Lagrangian advection computation. J Hydr Eng 1991;117:248–53.
[6] Karpik SR, Crockett SR. Semi-Lagrangian algorithm for two-dimensional advection–diffusion equation on curvilinear coordinate meshes. J Hydr Eng 1997;123:389–401.
[7] Stefanovic DL, Stefan HG. Accurate two-dimensional simulation of advective–diffusive-reactive transport. J Hydr Eng 2001;127:728–37.
[8] Ahmad Z, Kothyari UC. Time-line cubic spline interpolation scheme for solution of advection equation. Comput Fluids 2001;30:737–52.
[9] Knott GD. Interpolating cubic splines. Boston, New York: Birkhauser; 1991.
[10] Tsai TL, Yang JC, Huang LH. Characteristics method using cubic-spline interpolation for advection–diffusion equation. J Hydr Eng 2004;130:580–5.
[11] Tsai TL, Chiang SW, Yang JC. Characteristics method with cubic-spline interpolation for open channel flow computation. Int J Numer Methods Fluids 2004;46:663–83.